Acta Polytechnica **65**(2):252–262, 2025
https://doi.org/10.14311/AP.2025.65.0252

Published by the Czech Technical University in Prague

CONCEPTUAL DESIGN OF A SPACE NUCLEAR FAST REACTOR

Josef Sabol*, Jan Frýbort

Czech Technical University in Prague, Faculty of Nuclear Sciences and Physical Engineering, Department of Nuclear Reactors, V Holešovičkách 2, 180 00 Prague, Czech Republic

* corresponding author: saboljos@cvut.cz

Abstract. This paper finds an improved combination of fuel, enrichment, and coolant for a fast reactor suitable for nuclear electric propulsion. The study simulates an infinite lattice considering two enrichments, with fuel options (ceramics and metal alloys), and with alkali metals as a coolant. Following this, a simplified core model is developed to ensure long-term reactivity control and safe shutdown at a thermal power of 10 MW for 10 years, focusing on minimising size and mass.

The findings indicate two viable fuel and coolant combinations, depending on temperature requirements. For temperatures up to 1 100 K, the U-10Zr and Na combination is preferable due to its smaller critical dimensions and reduced mass. For higher temperatures, up to 1 550 K, the UN and Li combination is suitable. The choice of operating temperature is critical, as heat rejection in space depends only on radiation, covered by the Stefan-Boltzmann law, where heat flux depends on the fourth power of the temperature.

Keywords: Nuclear electric propulsion, space nuclear fast reactor, neutronic analysis, Serpent 2.

1. Introduction

The future of space exploration depends on the ability to travel further and more efficiently than ever before. To reach distant destinations in the Solar System within a reasonable time-frame, the availability of more powerful rocket engines capable of achieving the required speed is needed.

There are two basic types of propulsion systems. The first is chemical propulsion generating heat by a chemical reaction of the fuel to produce gases at high temperature and pressure. These gases expand and pass through a nozzle, creating thrust. Chemical engines are crucial for the initial phase of flight, providing the high thrust needed to bring a rocket into the Earth's orbit. However, due to the limited fuel supply, they can only operate for a short period of time. Additionally, a large portion of the rocket's launch mass consists of fuel, limiting its payload capacity.

The second type is electric propulsion, which uses electricity to ionize gases, creating thrust. Although the thrust generated by electric engines is insufficient for initial acceleration, these engines can operate for extended periods, making them suitable for long-term missions. Electric engines require a stable power source and a smaller amount of fuel compared to chemical engines, reducing the total fuel mass needed for the mission.

Sources of electricity for electric propulsion can include batteries, solar panels, or radioisotope generators. However, when high power in the magnitude of hundreds of kW is required, a nuclear reactor is the only viable option. Nuclear Electric Propulsion (NEP) uses thermal energy generated by the fission of nuclear fuel. This thermal energy is converted into electricity using thermocouples, Stirling engines, or turbines, which then drive the electric thruster to accelerate the rocket over an extended period [1].

When creating a space reactor, several limitations must be considered. The first is the limited size and the maximum payload mass that the rocket can carry into orbit. For smaller rockets, such as the Ariane 6 and Falcon Heavy, the payload fairing typically measures around 4.6 m in diameter and 14.5 m in height. These rockets can theoretically carry payloads of 11.5 t and 26.7 t, respectively, to Geostationary Transfer Orbit (GTO). Larger and more powerful rockets, such as the SLS Block 1B and Starship, have payload fairings with diameters ranging from 7.5 m to 8.0 m and heights of approximately 13 m, corresponding to payload capacities in the order of tens of tonnes [2–5].

The second limitation is heat dissipation. In space, cooling can only be achieved through radiation, which is covered by the Stefan-Boltzmann law:

$$\dot{Q}(S, T_2) = \sigma S(T_2^4 - T_1^4), \tag{1}$$

where

S denotes the radiator surface area,

T_2 denotes the thermodynamic temperature of the radiator,

T_1 denotes the thermodynamic temperature of space.

According to this equation, the heat rate depends on the fourth power of the temperature. For a constant heat rate dissipation, doubling the temperature allows for a reduction in the surface area of the radiator by a factor of 16. This relationship highlights the challenges of managing heat in the vacuum of space, where efficient thermal radiation is crucial for maintaining the reactor's operational stability.

Fuel	Theoretical density [g cm^{-3}]	Uranium Density [g cm^{-3}]	Melting Point [K]
UO_2	10.95	9.65	$3\,120 \pm 30$
UN	14.33	13.54	$3\,123 \pm 30$
UC	13.50	12.85	$2\,780 \pm 25$
U-10Mo	17.20	15.48	1 473
U-10Zr	16.31	14.70	1 633

TABLE 1. Basic parameters of five selected fuel types. Density is given at 25 °C. Taken from [6–8].

Liquid metal cooled fast reactors are certainly a viable option due to the requirement of small dimensions and weight, high power density, and high operating temperature. This choice is also justified by historical precedence. The Soviet Union was a significant pioneer in this field, launching 33 fast nuclear reactors satellites into orbit between 1970 and 1988. In contrast, the United States sent only one epithermal reactor, the SNAP-10A. It is important to note that none of these reactors functioned as NEPs; they were used only as power sources for on-board electronics [9].

In the 1990s, the United States attempted to revive this research with the SP-100 project, which serves as the primary design basis for this paper [10]. However, like many later projects, it was canceled after a few years. Today, the concept is being revisited, with a significant shift: both NASA and ESA are now relying on greater involvement of the private sector and the integration of new technologies [11, 12].

The aim of this paper is not to find the optimal materials in terms of neutronics, thermodynamics, and chemical processes. Instead, it focuses on the conceptual design of a small and lightweight compact nuclear reactor operated in fast neutron spectrum for space applications. At this stage, only the basic materials for fuel, coolant, reflector, and cladding will be considered. For the full-core calculations, the requirement of a constant thermal output of 10 MW for 10 years will be assumed.

It is important to note that this analysis neglects several important factors and defer them to a later stage. These factors include material properties (elasticity and strength), chemical reactions (material oxidation), brittleness due to cosmic rays and neutron flux, thermomechanical properties due to burnup, and many other factors. If the aim was to design a reactor for a real space mission, more detailed testing of different materials would be required, which might lead to different choices. Nevertheless, these simplified approaches can provide useful insights and shape further development.

2. Computational tools & statistical settings

All calculations are based on the stochastic Monte-Carlo transport code Serpent 2 version 2.2.0 [13] and the nuclear data library ENDF/B-VIII.0 [14]. For the infinite lattice calculations, 10 000 simulated particles in 500 active cycles and 100 inactive cycles were used. For the basic full-core calculations, 10 000 particles in 1 500 active and 100 inactive cycles were considered.

This statistical setting leads to a multiplication factor uncertainty of about 15 pcm.

When calculating the fuel depletion using the predictor-corrector method, the 10-year time interval was divided into segments of 1 day, 2 days, and 5 days initially, followed by intervals of 1 year for the remaining duration of up to 10 years. This approach was used to sufficiently stabilise the concentration of short-lived fission products and accurately determine the neutron flux evolution.

3. Materials

There are many different combinations available. However, in this work, special consideration is given to five basic and most frequently considered fuel types, alkali metal coolants, neutron absorbing elements based on the ^{10}B isotope, and a reflector based on the ^{9}Be isotope.

Most of thermophysical properties of materials have been considered according to the IAEA collection of data correlations [6]. Data for U-10Mo alloy were taken from [7], for U-10Zr alloy from [8] and for Mo-14Re alloy from [15, 16].

3.1. Fuel

Five fuel types will be considered, namely:

- ceramic fuels (UO_2, UN and UC) – higher melting point, lower uranium content;
- metallic fuels (10 % wt. Mo and Zr) – lower melting point, higher uranium content.

The basic parameters are given in Table 1. For higher excess reactivity and to achieve a smaller critical volume, fuels with higher uranium content, such as metallic fuels, are suitable. However, they also have a lower melting temperature (around 1 500 K), which is problematic for reactors operating at high output temperatures due to the risk of severe accidents. In contrast, ceramic fuels exhibit higher melting temperatures but contain less uranium, resulting in lower excess reactivity and requiring a larger critical volume.

Nuclear fuel thermodynamic properties are also important, especially the thermal conductivity, which affects the temperature gradient in the block of fuel.

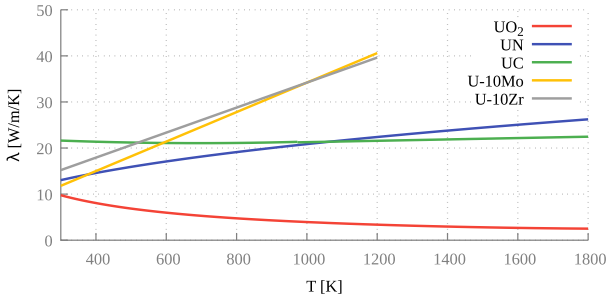

Figure 1. Temperature dependence of thermal conductivity for five selected fuel types. The graph includes various correlations that vary depending on factors, such as porosity or contamination levels. It is, therefore, for illustrative purposes only [6–8].

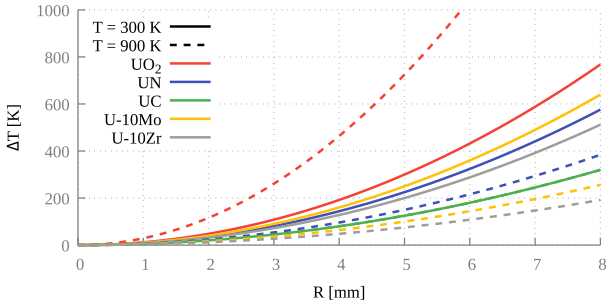

Figure 2. Temperature gradient between the centre and the surface of the fuel rod for five selected fuel types and for two mean temperatures at power density $q_V = 500\,\mathrm{W\,cm^{-3}}$. Temperature expansion is not considered. The curves for UC merged together due to only a negligible difference.

The higher the thermal conductivity, the smaller is the difference between the centre of the rod and the surface. The change in thermal conductivity with temperature is shown in the graph in Figure 1. It is clear that for metallic fuels, it increases significantly with temperature, while for ceramic fuels, the changes are more gradual.

Consider a model example of a fuel rod with power density $q_V = 500\,\mathrm{W\,cm^{-3}}$ (this is the approximate power density as in PWRs). Considering the 1D Fourier heat equation in cylindrical coordinates, the temperature drop between the surface and the maximum at the centre of the rod can be described by:

$$\Delta t(R) = \frac{q_V}{4\lambda} R^2. \qquad (2)$$

Neglecting volume expansion, the power density can be considered constant, and the only parameter dependent on temperature change is the thermal conductivity. The graph in Figure 2 shows the calculated temperature differences between the centre and the surface of the rod for two mean temperatures: 300 K and 900 K.

The highest temperature gradient is observed for the most common fuel form, UO_2, while the lowest gradient occurs for UC fuel. This trend changes at higher temperatures, where metallic fuels dominate due to their higher thermal conductivity.

A final consideration in proper fuel selection is the accompanying composition of the remaining nuclides and their effect on parasitic neutron absorption. Special attention should be paid to N, as other elements, such as O, C, Mo, and Zr, are not very dominant in neutron absorption.

Nitrogen consists of two stable isotopes, ^{14}N and ^{15}N, in a mass ratio of approximately 250:1. From the neutron capture point of view, the isotope ^{14}N is significant due to its (n,p) and (n,γ) reactions. This requires the enrichment of natural nitrogen for use in UN fuel.

3.2. Coolant

Fast reactors need to be cooled with coolants that do not slow-down neutrons and are fluids at high operating temperatures. Usually gases, salts, or molten metals are considered for high-temperature systems. Another consideration is their specific heat capacity, indicating how much heat they can absorb when heated by 1 K. Molten salts and liquid metals are advantageous in this characteristic allowing for higher power density, lower mass flow to cool the core, thus reducing potentially pressure losses.

Coolant	Melting point [K]	Boiling point [K]
Li	454	1 620
Na	371	1 156
K	337	1 047
Na-78K	261	1 057

Table 2. Basic parameters of alkali metals [6–8].

This work will focus on cooling using only liquid alkali metals, although the choice of other coolants (e.g. FLi and FLiBe salts or the eutectic alloy Pb-56Bi) would also be justified. If the study is to be continued, it would be worthwhile to consider other alternatives.

Table 2 shows the melting and boiling temperatures for alkali metals and for the eutectic Na-78K. It can be seen that the temperatures gradually decrease with increasing period[1]. Thus, for high-temperature reactors, it is appropriate to use Li for cooling, whereas for lower temperatures cooling using Na-78K would be sufficient. However, a major disadvantage of alkali metals is their strong oxidation reaction with water, but it is not an issue for a system in space.

In addition to the melting and boiling points, density (see Figure 3) and heat capacity (see Figure 4) are also important. This implies, for example, that 1 kg of liquid Li can dissipate the most heat, but it also occupies the largest volume compared to other metals, which may have a negative impact on the need for higher flows or a larger temperature gradient at the reactor inlet and outlet.

[1] Period in the periodic table of elements.

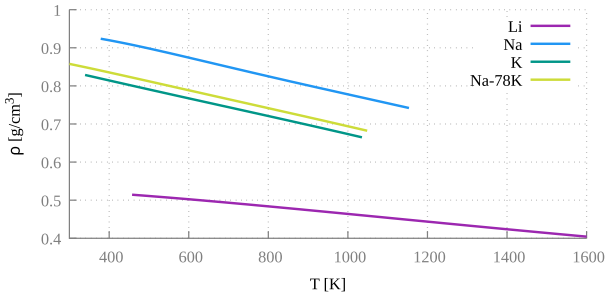

FIGURE 3. Density dependence on temperature for selected alkali metals [6–8].

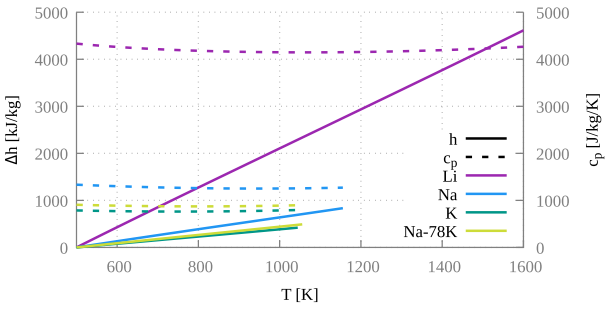

FIGURE 4. Temperature dependence of specific heat capacity and enthalpy change for selected alkali metals. The enthalpy change is related to 500 K [6–8].

Consider again the model example of power dissipation $\dot{Q}$ by area S when the coolant is heated by 1 K. Then, after applying the continuity equation for incompressible liquids and the calorimetric equation, the required mean flow velocity can be calculated by:

$$\bar{v}(T) = \frac{\dot{Q}}{\bar{\varrho}(T)\, S\, \bar{c_p}(T)\, \Delta t}, \tag{3}$$

which is also demonstrated by the graph in Figure 5. It can also be seen that if velocity is the only characteristic to compare, it is not necessary to quantify the values of $\dot{Q}$ and S. Thus, this calculation is again in favour of Li. When heated by 1 K at constant power and with a constant area, the smallest velocity is needed. At the same time, the curve is the most constant of all, so the velocities at the reactor inlet and outlet will be most similar. This is followed by Na, while the worst results will be obtained with K.

The last parameter is the parasitic neutron absorption, which is a disadvantige for Li. It is a natural mixture of two isotopes ^{6}Li and ^{7}Li in a mass ratio of approximately 1:14.2. While the (n,γ) reaction is very similar for both isotopes, the (n,t) reaction is much more dominant for ^{6}Li. Thus, some level of Li enrichment is necessary.

3.3. Other materials

The **Neutron reflector** will be based on beryllium in the form of BeO with a density of 3.01 g cm^{-3} and with a melting point of 2 823 K. Beryllium is an effective neutron reflector with low parasitic absorption.

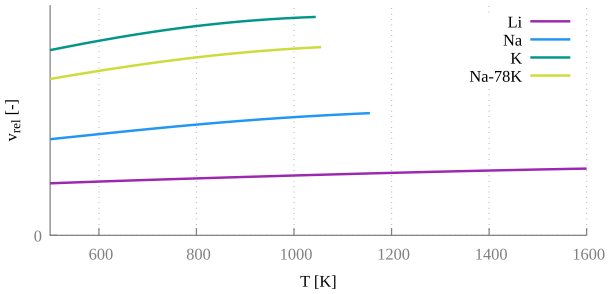

FIGURE 5. Comparison of the relative velocities required to heat by 1 K at constant power while passing through a constant area for selected alkali metals.

The **Neutron absorber** will be boron in the form of B_4C with a density of 2.51 g cm^{-3} and a melting point of 2 723 K. Boron consists of two stable isotopes, ^{10}B and ^{11}B, with a mass distribution of approximately 1:4. For neutron absorption, the isotope ^{10}B is dominant, mainly due to the (n,α) reaction. It is, therefore, advisable to enrich natural boron, in this case up to 90 %.

The only structural material considered will be the **fuel cladding**. There are three basic cladding requirements: low parasitic absorption, high melting temperature, and good thermal conductivity. There is a lot of different alloys, steels, ceramics or other composite materials available. For this work, Mo-14Re alloy with a density of 10.93 g cm^{-3} was selected, which is characterised by high melting temperature (approximately 2 900 K), good thermal conductivity (on the magnitude of tens of W m^{-1} K^{-1}), and low parasitic absorption. This alloy has also appeared several times in the past in other high-temperature reactor designs for space applications, for example, the SP100 design [10] mentioned in the Introduction, which was the main reason of this selection.

4. Infinite lattice study

An infinite lattice calculation was performed to select the appropriate fuel, coolant and pitch. In terms of cooling, Li and Na appear to be the best, each allowing operation at different temperatures. For this purpose, two reference temperatures will be considered: 600 K for Na and 1 200 K for Li. The cladding temperature will be the same as the coolant temperature, while the fuel temperature will be 300 K higher. This deviation should correspond to an order of magnitude temperature drop as shown in Figure 2.

In total, there are 8 different fuel and coolant combinations, which are shown in Table 3. The lattice geometry was chosen to be triangular with the fuel rod parameters: 5 mm radius, 5.15 mm inner and 5.75 mm outer radius of the fuel cladding. The gap between the fuel and the cladding was filled with vacuum, although in practice, helium would probably be used. There is only a negligible effect on the neutron behaviour.

The values of a pin pitch were selected from a range of 1.2 cm to 3.0 cm. However, fast reactors are charac-

Fuel	Fuel temperature [K]	Cladding temperature [K]	Coolant	Coolant temperature [K]
UO_2	900	600	Na	600
UN	900	600	Na	600
UC	900	600	Na	600
U-10Mo	900	600	Na	600
U-10Zr	900	600	Na	600
UO_2	1 500	1 200	Li	1 200
UN	1 500	1 200	Li	1 200
UC	1 500	1 200	Li	1 200

Table 3. Fuel and coolant combinations considered.

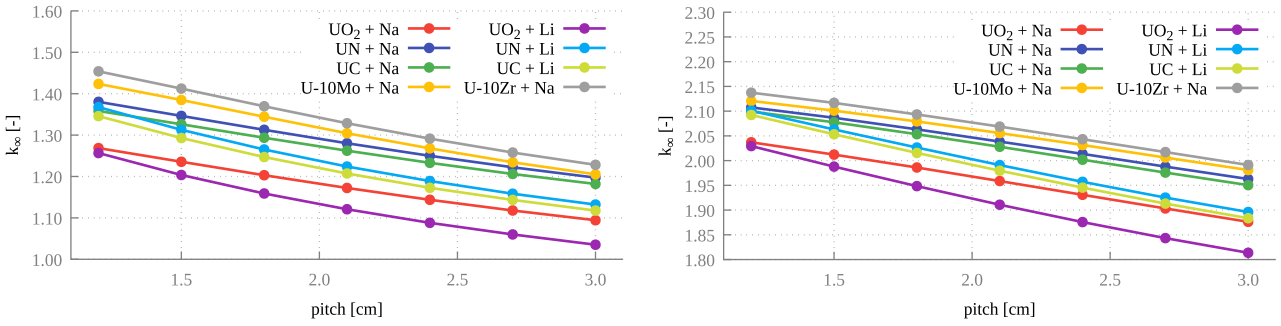

(a). HALEU fuel.

(b). HEU fuel.

Figure 6. Excess reactivity for an infinite lattice calculation.

terised by a large migration area, which means that neutrons travel a much greater distance between the creation and destruction than in the case of thermal reactors. Therefore, the fuel/coolant ratio is much more important. From a thermodynamic point of view, it is advisable to choose a fuel radius that minimises the temperature gradient between the centre and the surface, and at the same time choose a flow area for the coolant that minimises pressure losses due to higher flow speeds. A radius of 5 mm was then chosen because it is relatively easy to manufacture on an industrial scale.

All densities and dimensions were considered at a room temperature of 25 °C, and thermal expansion was neglected. Density variation was considered only in the case of the coolant.

As mentioned in the previous chapter, enrichment is necessary when using UN fuel and Li coolant. The calculations carried out show that enrichment to the level of 95 % ^{15}N or 99.9 % ^{7}Li is sufficient, as there were no significant reactivity changes beyond these values.

Two types fuel enrichment were considered. Namely HALEU fuelenriched to 19.75 % and HEU fuel, which is highly enriched uranium enriched to 90 %. The HALEU fuel with enrichment below 20 % is the most important, as this is the limit of enrichment for Gen-IV reactors and SMRs. It is interesting to look at higher enrichments, and although 90 % enrichment is too high, it is interesting to see how small the reactor could be.

The graphs in Figure 6 show the infinite lattice calculations for HALEU and HEU fuel. In both cases, it is clear that the excess reactivity corresponds directly to the partial density of uranium in the material. Thus, it is the highest for the U-10Zr fuel and the lowest for the UO_2 fuel. It is also shown that the use of Na as a coolant is preferable to Li in terms of excess reactivity. This difference gradually increases with higher pitch, as this also increases the ratio of the coolant in the system.

The excess reactivity also corresponds to the fuel enrichment. It is the highest for the HEU fuel, which can easily be operated in the fast spectrum. The HALEU fuel is also supercritical, but has a lower reactivity, so a larger system with a limited leakage will be necessary.

5. Full-core study & depletion

5.1. Geometry description

The geometry is simplified. It consists of fuel rods, which are axially divided into these parts: the lower reflector part, the fuel part, the gas plenum for fission product accumulation, and the upper reflector part. Each fuel rod is enclosed in a cladding with dimensions presented in the previous section. Other components, such as the cooling circuit, pumps, shielding, etc. are not included in this analysis, since the study focuses only on basic neutronic analysis.

A radial reflector of the same thickness as the upper and lower axial reflectors is attached to the core. The gas plenum has a fixed length of 2 cm. Other

Configuration	Number of Fuel Rods	Number of Safety Rods
HALEU	2 202, $R = 5\,\mathrm{mm}$	55, $R = 6\,\mathrm{mm}$
HEU	456, $R = 5\,\mathrm{mm}$	55, $R = 7\,\mathrm{mm}$

TABLE 4. Basic configuration of selected reactors.

parameters, such as pin pitch, number of rods, length of the fuel section, and thickness of the reflector are optional and can be varied as required. The space between the rods is filled with coolant. A simplified drawing is shown in Figure 9 in the Appendix.

Power regulation is provided by 12 rotating drums with cut-outs of absorber located in the radial reflector. With the help of drum rotation, it is possible to influence the excess of neutrons in the system and thus regulate the power and the loss of reactivity due to depletion. For emergency shutdown, safety rods are used, which can be inserted in vacant positions in place of the fuel rods.

During the analysis, efforts will be made to meet the following parameters:

- minimal volume along with minimal mass;
- the ability to completely shutdown the reactor during operation with the help of safety rods;
- sufficient excess reactivity to operate at a thermal power of 10 MW and an operating time of 10 years (with $k_{\mathrm{eff}} \approx 1.01$ at EOL);
- maximum coolant flow velocity of $2\,\mathrm{m\,s^{-1}}$;
- coolant temperature gradient between inlet and outlet set to 50 K or 100 K;
- reasonable specific power (maximum up to $50\,\mathrm{kW\,kg_{HM}^{-1}}$);
- maximum burnup up to $150\,\mathrm{MW\,d\,kg_{HM}^{-1}}$.

The last four parameters are crucial in terms of thermal hydraulics. While it is possible to operate liquid metal cooled fast reactors at higher temperature gradients (up to 150 K), higher power densities, and higher flow velocities (in the magnitude of higher units of $\mathrm{m\,s^{-1}}$), in this case, since it is a space system, the thermal hydraulic parameters will be kept at lower conservative values.

5.2. Reactivity control and shutdown system

The absorbing material is B_4C with 90 % enrichment of ^{10}B. For power control, 12 rotating control drums in a radial reflector with a 2 cm cut-outs from the absorber are used. For a 10 cm thick reflector, the cylinders are 9.5 cm in diameter, for a 15 cm thick reflector, the cylinders are 14.5 cm in diameter. The control works by reducing the absorption of neutrons in the periphery in the "out" position (absorber outside the core), which increases the reflectivity from the reflector itself, and thus the reactivity. Conversely, in the "in" position (absorber closest to the core), the leaking neutrons are absorbed, reducing the reflectivity, and thus reactivity. The advantage of this control system is that it allows control over the entire axial length of the core, not just the top part as in the case of control rods.

Safety rods are used to safely shutdown the reactor (and also for safe subcritical transport during launch to the orbit) and will be inserted into vacant positions in the core. Their diameter can be greater than that of the rods, but they need to fit in the lattice. At the same time, a sufficient number of rods must be available to safely shutdown the reactor in any situation during operation, even if some rods fail. Each of these rods will have the possibility of being connected to an independent system (e.g. spring, compressed gas) which will be activated in the event of a safety circuit tripping and the rod will be inserted into the core regardless of gravity or other acceleration.

5.3. Critical dimensions

According to the calculations, 2 combinations come out best from an infinite lattice:

- U-10Zr & Na combination for 900 K;
- UN & Li combination for 1 200 K.

In terms of achieving higher thermal efficiency for the secondary power generation system, and for the better heat removal system, it is preferable to select a higher temperature for the primary part (i.e. UN & Li). The U-10Zr & Na combination achieves a higher excess reactivity and should potentially lead to a reduction in critical volume. However, in terms of mass, it is important to note that both Na and U-10Zr achieve higher densities, which means that a smaller volume does not necessarily mean a smaller mass. For this reason, it is advisable to consider both combinations in the next selection step.

For HEU fuel, the core can be smaller. Overall, the use of 456 fuel rods and 55 safety rods with 17 mm pitch and 10 cm reflector thickness is appropriate. For HALEU fuel, it is necessary to enlarge the core due to neutron leakage and choose a thicker reflector with a thickness of 15 cm. The best choice is to use 2 202 fuel rods and 55 safety rods. Because of the lower power density, a smaller pitch of 13 mm can be chosen. The height of the core then depends on the specific fuel & coolant combination, with all parameters available in Tables 4 and 5. The radial cross section for both systems is shown in Figure 10 in the Appendix.

Configuration	Pitch [mm]	Core Height [cm]	Core Radius [cm]	Reflector Thickness [cm]	Mass [kg]
HALEU: U-10Zr & Na	13	70	33.15	15	3 900
HALEU: UN & Li	13	92	33.15	15	4 500
HEU: U-10Zr & Na	17	47.25	21.25	10	760
HEU: UN & Li	17	52	21.25	10	755

Table 5. Specific dimensions and mass of selected reactors.

Configuration	Specific Power $[\mathrm{kW\,kg_{HM}^{-1}}]$	Maximum Burnup $[\mathrm{MW\,d\,kg_{HM}^{-1}}]$
HALEU: U-10Zr & Na	5.6	20.6
HALEU: UN & Li	4.6	17.0
HEU: U-10Zr & Na	40.3	147.0
HEU: UN & Li	39.7	144.9

Table 6. Basic energy parameters of selected reactors.

Configuration	$\dot{m}$ $[\mathrm{kg\,s^{-1}}]$	$\bar{v}$ $[\mathrm{m\,s^{-1}}]$	Re [-]	$\dot{m}$ $[\mathrm{kg\,s^{-1}}]$	$\bar{v}$ $[\mathrm{m\,s^{-1}}]$	Re [-]
	$\Delta T = 50\,\mathrm{K}$			$\Delta T = 100\,\mathrm{K}$		
HALEU: U-10Zr & Na	153.6	1.9	24 100	76.9	0.9	12 100
HALEU: UN & Li	48.1	1.2	11 200	24.1	0.6	5 600
HEU: U-10Zr & Na	153.6	2.6	116 200	76.9	1.3	58 200
HEU: UN & Li	48.1	1.6	54 100	24.1	0.8	27 100

Table 7. Basic thermal hydraulic parameters of coolant for selected reactors. The table contains 2 sets of values for a temperature drop between inlet and outlet of 50 K and 100 K respectively.

5.4. Thermal hydraulic calculations

The thermal hydraulic calculation was carried out based only on the basic balance equation of the conservation of energy and mass flow. In the case of HEU fuel, the specific power is approximately $40\,\mathrm{kW\,kg_{HM}^{-1}}$ and the maximum burnup after 10 years is up to $150\,\mathrm{MW\,d\,kg_{HM}^{-1}}$, which is sufficient. In the case of HALEU fuel, the values are about 8 times smaller due to the larger core (see Table 6).

When converted to the parameters of the coolant required for cooling (see Table 7), the required flow velocity is approximately $2\,\mathrm{m\,s^{-1}}$ in the case of a 50 K temperature drop and approximately $1\,\mathrm{m\,s^{-1}}$ in the case of a 100 K drop. In this respect, the UN & Li combination works much better for the reasons discussed in the previous material section.

In terms of pressure loss, the Reynolds number, which characterises the nature of the flow (laminar vs. turbulent), also shown in Table 7, plays a major role. Here it can be seen that due to the larger flow area, the Reynolds number for HEU fuel is up to 5-times higher. In addition, the combination of UN & Li gives half the Reynolds number, also, a temperature drop of 100 K, which is due to roughly half the flow speed. Thus, in terms of potential pressure losses, the UN & Li combination is indeed the most suitable.

During the calculation, it was assumed that each fuel rod generates the same amount of heat and neglects pin power peaking. It is, therefore, advisable to stick to lower conservative values. For this reason, the flow area considered was reduced to only the area surrounding the fuel rods in each of the reactor lattice cells. The coolant flowing in the periphery or through the free channels for the safety rods was not included in the calculation.

5.5. Reactivity during depletion

The graphs in Figure 7 show the multiplication factor during depletion for the maximal reactivity (drums and rods in the "out" position), for the case with drums in the "in" position and for the case with rods in the "in" position. Clearly, in the case of drums in the "in" position, the reactor is subcritical in all cases, so the drums can be used for reliable control. At the same time, if the rods are inserted in the core, then $k_{\mathrm{eff}} < 0.95$ in all cases, which is a sufficiently subcritical bound.

Comparing the U-10Zr & Na and UN & Li combinations, it can be seen that the latter achieves deeper subcriticality for both HEU and HALEU fuel cases. Therefore, the UN & Li combination is preferable in this respect, as the reactivity worths of the control and shutdown systems are greater.

5.6. Neutron spectrum

The graphs in Figure 8 show that in all cases, this is a pure fast reactor. In the case of U-10Zr & Na, the spectrum is even slightly harder.

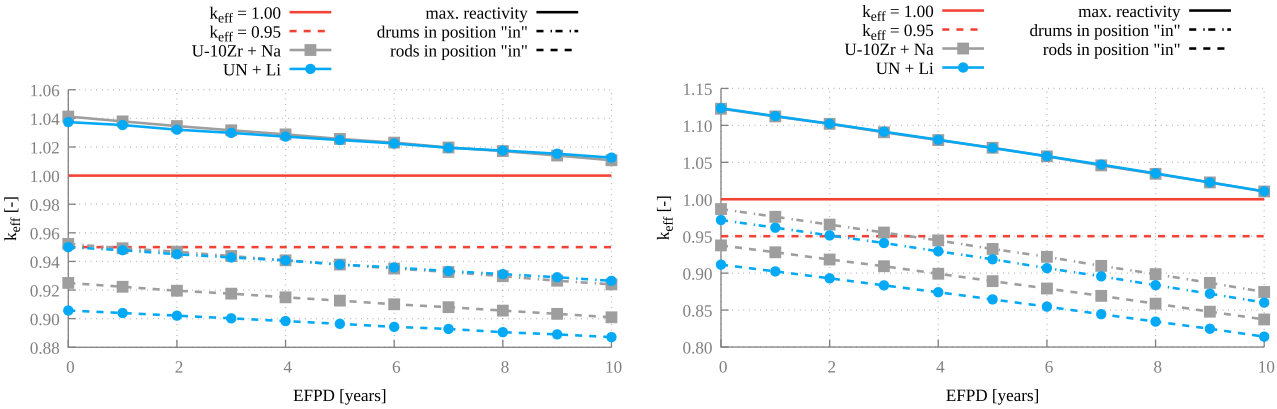

(A). HALEU fuel. (B). HEU fuel.

FIGURE 7. Reactivity during depletion.

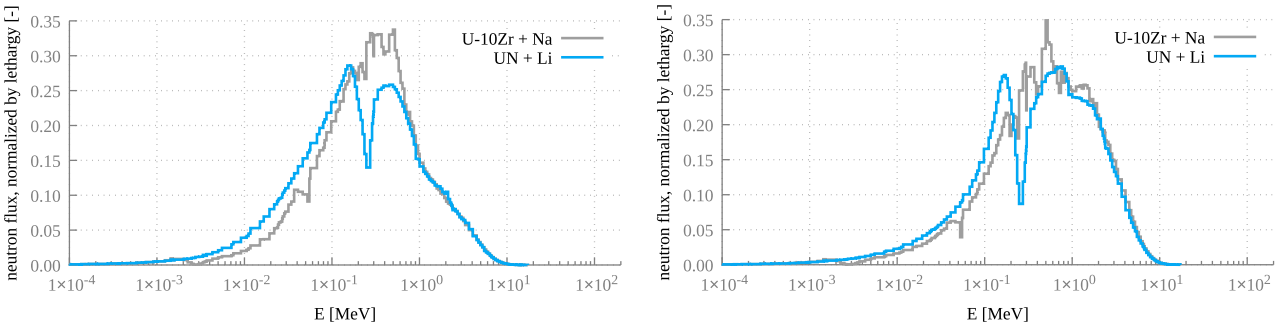

(A). HALEU fuel. (B). HEU fuel.

FIGURE 8. Neutron spectrum in the fuel.

Configuration	ϕ^{f} [%]	ϕ^{th} [%]	F^{f}_{fiss} [%]	F^{th}_{fiss} [%]
HALEU: U-10Zr+Na	98.7	1.3	36.7	63.3
HALEU: UN+Li	98.8	1.2	36.7	63.3
HEU: U-10Zr+Na	99.9	0.1	34.0	66.0
HEU: UN+Li	99.9	0.1	33.2	66.8

TABLE 8. Comparison of neutron flux and fission reaction rate for selected reactors at BOL.

The same is shown in Table 8, which compares fast and thermal neutron fluxes and reaction rate values for fission between the fast and the thermal versions. In the case of the neutron flux, the ratio is as high as 99 % in favour of the fast group, and as high as 99.9 % in the case of HEU fuel (the HEU system is even smaller and the large migration area does not allow neutrons to lose as much energy). However, the fission reaction rate is still greater for the thermal group due to several orders of magnitude difference in the microscopic fission cross section in favour of the thermal group.

6. Conclusion

The aim of the paper was to find suitable combinations of enrichment, fuel type, and coolant type for a fast nuclear space reactor with special emphasis on minimum size, mass, and high outlet temperature.

First, the selected materials were described. Three representatives of ceramic composites (UO_2, UN and UC), which are characterised by lower thermal conductivity, lower uranium density, but high melting point, and representatives of metal alloys (U-10Mo and U-10Zr) with 10 % wt. of secondary metal admixture, for which, conversely, higher thermal conductivity and higher uranium density, but lower melting temperature apply, were chosen. Only alkali metals were considered as coolants, and only sodium and lithium were selected for further study in terms of basic thermal hydraulic properties. BeO was chosen as the material for the reflector, 90 % enriched B_4C for the absorber, and Mo-14Re alloy as the structural material for the cladding. In Addition, two levels of enrichment were considered: uranium enriched up to 20 % (HALEU) and high enrichment to 90 % (HEU).

These materials were used in the next step for the basic neutronic calculation in an infinite lattice for the 2 coolants considered and for the 2 reference temperatures. These were 600 K for sodium and 1 200 K

for lithium, with all five fuel types used for sodium cooling, while only ceramic fuels were used for lithium cooling. As a result, the best results in terms of excess reactivity can achieved using the combination of U-10Zr & Na for 600 K and UN & Li for 1 200 K.

The next step was to perform a full-core calculation only for the two combinations mentioned above and for both enrichments. Here, it turned out that the combination of U-10Zr & Na performs slightly better dimensionally for both enrichments and mass-wise for the HALEU fuel, however, for the HEU fuel, both combinations weigh about the same. Reactivity control consisted of 12 rotating control drums with cut-outs from the absorber in the radial reflector and safety rods occupying empty positions in the fuel lattice for a safe shutdown.

The full-core calculation also included a simplified thermal hydraulic calculation. This was carried out using the basic energy balance equation and the continuity equation. Here, it was found that for a temperature drop of 50 K between the inlet and outlet, the coolant must move at a velocity of approximately $2\,\mathrm{m\,s^{-1}}$, while for a temperature drop of 100 K, it must move at approximately $1\,\mathrm{m\,s^{-1}}$. The aspect of potential pressure loss was investigated by calculating only the Reynolds number, which comes out up to 2-times smaller for the UN & Li combination and up to 5-times smaller for the HALEU fuel.

As a result, it turns out that the U-10Zr & Na combination achieves smaller size and mass, however, in terms of cooling, the UN & Li combination is preferable. The enrichment comparison shows that smaller size and mass can be achieved using HEU fuel, however there would be a higher pressure loss.

As mentioned in the Introduction, only radiation can be used to dissipate heat in space. At low power levels, this should not be a problem, but when considering power dissipation in units of MWs, temperature plays a huge role. Theoretically, it would be possible to operate a sodium reactor at a temperature of 1 100 K and a lithium reactor at temperature of a 1 550 K, while this temperature difference could make up to a 4-fold difference in the required radiator area.

Another question would be whether a moderated thermal or epithermal system would be more appropriate for HALEU fuel, which could lead to a reduction in size, and therefore a reduction in mass. The study of both issues should be the subject of further follow-up work.

In conclusion, this work has dealt with neutronic analysis, i.e. how the given combination of materials relates to each other, and at the same time has focused on only 5 types of fuel, one type of cladding, and alkali metal cooling. If it is planned to extend the article from a conference paper to a journal paper, it would be appropriate to supplement this selection with other materials, such as ceramic cladding (SiC), cooling with molten salts (FLiBe or FLi) or other liquid metals (Pb, Pb -56Bi), or different types of fuel.

At the same time, the work does not deal in detail with the thermal hydraulic study and the burnup possibilities. It is not certain whether the cladding or the fuel itself can withstand such burnup, what their chemical compatibility is, or how the system would behave if thermal expansion were taken into account. It would also be useful to compare these results with experimental data. However, this is also a possible topic for the future.

List of symbols

B Burnup $[\mathrm{MW\,d\,kg^{-1}}]$
c_p Specific heat capacity $[\mathrm{J\,kg^{-1}\,K^{-1}}]$
D Diameter [cm]
E Energy [MeV]
F Reaction rate $[\mathrm{cm^{-3}\,s^{-1}}]$
H Height [cm]
h Specific enthalpy $[\mathrm{kJ\,kg^{-1}}]$
k Multiplication factor [–]
m Mass [kg, g]
$\dot{m}$ Mass flow rate $[\mathrm{kg\,s^{-1}}]$
P Power [W]
R Radius [cm]
S Area $[\mathrm{cm^2}]$
Q Heat [J]
$\dot{Q}$ Heat flow rate [W]
q Specific power $[\mathrm{kW\,kg^{-1}}]$
q_V Power density $[\mathrm{W\,cm^{-3}}]$
T Thermodynamic temperature [K]
t Temperature [°C]
V Volume $[\mathrm{cm^3}]$
v Velocity $[\mathrm{m\,s^{-1}}]$
ϕ Neutron flux $[\mathrm{cm^{-2}\,s^{-1}}]$
λ Thermal conductivity $[\mathrm{W\,m^{-1}\,K^{-1}}]$
ϱ Density $[\mathrm{g\,cm^{-3}}]$
ρ Reactivity [pcm]
σ Stefan–Boltzmann constant $[\mathrm{W\,m^{-2}\,K^{-4}}]$
Re Reynold's number

BOL Beginning of life
EOL End of life
EFPD Effective full power day
HALEU High-assay low-enriched uranium
HEU Hight-enriched uranium
HM Heavy metal
fiss Fission
f Fast group
th Thermal group

References

[1] D. Buden. *Space nuclear propulsion and power: Space nuclear fission electric power systems.* Polaris Books, 2011. ISBN 9780974144344.

[2] Arianespace. *Ariane 6 user's manual. Issue 2, Revision 0*, 2021. [2024-06-20]. https://www.arianespace.com/wp-content/uploads/2021/03/Mua-6_Issue-2_Revision-0_March-2021.pdf

[3] SpaceX. *Falcon user's guide*, 2021. [2024-06-20]. https://www.spacex.com/media/falcon-users-guide-2021-09.pdf

[4] NASA. Space launch system lift capabilities. [2024-06-20]. https://www.nasa.gov/wp-content/uploads/2020/02/sls_lift_capabilities_and_configurations_508_08202018_0.pdf

[5] SpaceX. Starship. [2024-06-20]. https://www.spacex.com/vehicles/starship/

[6] International Atomic Energy Agency. *Thermophysical properties of materials for nuclear engineering: A tutorial and collection of data*. 2008. [2024-06-20]. https://www-pub.iaea.org/MTCD/Publications/PDF/IAEA-THPH_web.pdf

[7] J. Rest, Y. S. Kim, G. L. Holmes, et al. U-Mo fuels handbook, version 1.0. Tech. Rep. ANL-09/31, Argonne National Laboratory, 2006. [2024-06-20]. https://publications.anl.gov/anlpubs/2009/12/65696.pdf

[8] D. E. Janney. *Metallic fuels handbook, Part 1: Alloys based on U-Zr, Pu-Zr, U-Pu, or U-Pu-Zr, including those with minor actinides (Np, Am, Cm), rare-earth elements (La, Ce, Pr, Nd, Gd), and Y*. Idaho National Laboratory, 2017. [2024-06-20]. https://inldigitallibrary.inl.gov/sites/sti/sti/Sort_2909.pdf

[9] World Nuclear Association. Nuclear reactors and radioisotopes for Space, 2021. [2024-06-20]. https://world-nuclear.org/information-library/non-power-nuclear-applications/transport/nuclear-reactors-for-space

[10] S. F. Demuth. SP100 space reactor design. *Progress in Nuclear Energy* **42**(3):323–359, 2003. https://doi.org/10.1016/S0149-1970(03)90003-5

[11] ESA. Space transportation and nuclear propulsion, 2022. [2024-06-20]. https://commercialisation.esa.int/2022/09/space-transportation-and-nuclear-propulsion/

[12] NASA. Nuclear propulsion could help get humans to Mars faster, 2021. [2024-06-20]. https://www.nasa.gov/solar-system/nuclear-propulsion-could-help-get-humans-to-mars-faster/

[13] J. Leppänen, M. Pusa, T. Viitanen, et al. The Serpent Monte Carlo Code: Status, development and applications in 2013. *Annals of Nuclear Energy* **82**:142–150, 2015. https://doi.org/10.1016/j.anucene.2014.08.024

[14] D. A. Brown, M. B. Chadwick, R. Capote, et al. ENDF/B-VIII.0: The 8$^{\text{th}}$ major release of the nuclear reaction data library with CIELO-project cross sections, new standards and thermal scattering data. *Nuclear Data Sheets* **148**:1–142, 2018. https://doi.org/10.1016/j.nds.2018.02.001

[15] Future alloys. Molybdenum – datasheet. [2024-06-20]. https://futurealloys.co.uk/molybdenum-data-sheet/

[16] ESPI Metals. Rhenium. [2024-06-20]. https://www.espimetals.com/index.php/technical-data/191-Rhenium

Appendix A.

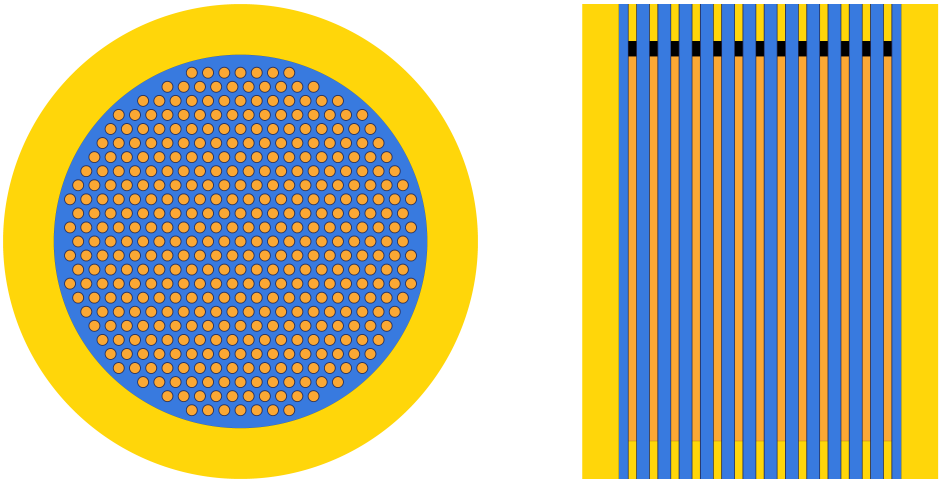

(a). Radial cross section. (b). Axial cross section.

Figure 9. Example of the model.

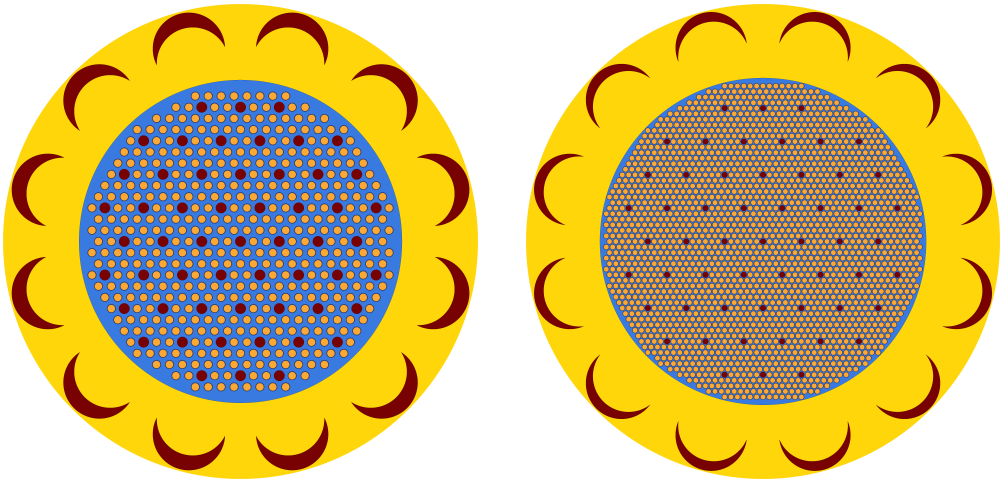

(a). HEU fuel. (b). HALEU fuel.

Figure 10. Radial cross section of the reactor model (both images are to the same scale relative to each other).